Published in final edited form as:
Biomaterials. 2008 January ; 29(1): 33–46. doi:10.1016/j.biomaterials.2007.08.045.

DIFFERENCES BETWEEN THE EFFECT OF ANISOTROPIC AND ISOTROPIC LAMININ AND NERVE GROWTH FACTOR PRESENTING SCAFFOLDS ON NERVE REGENERATION ACROSS LONG PERIPHERAL NERVE GAPS

Mahesh Chandra Dodla and **Ravi V. Bellamkonda***
Neurological Biomaterials and Therapeutics, Wallace H. Coulter Department of Biomedical Engineering, Georgia Institute of Technology/Emory University, Atlanta Georgia 30332

Abstract

Anisotropic scaffolds of agarose hydrogels containing gradients of laminin-1 (LN-1) and nerve growth factor (NGF) molecules were used to promote sciatic nerve regeneration across a challenging 20 mm nerve gap in rats. Step and continuous gradient anisotropic scaffolds were fabricated and characterized and regeneration was compared to that in isotropic scaffolds with uniform concentrations of LN-1 and NGF and sciatic nerve grafts harvested from syngenic rats. Polysulfone tubular guidance channels were used to present the agarose based scaffolds to the nerve stumps. Four-months after implantation, regenerating axons were observed in animals implanted with anisotropic scaffolds with gradients of both LN-1 and NGF molecules and nerve grafts, but not in animals with isotropic scaffold implants. Also, the scaffolds with gradient of either LN-1 or NGF, with the other component being uniformly distributed in the scaffold, did not elicit axonal regeneration. The total number of myelinated axons was similar for the anisotropic scaffold and the nerve graft conditions, with the anisotropic scaffolds having a higher density of axons than the nerve grafts. Axonal diameter distribution was similar for the anisotropic scaffolds and the nerve grafts. The nerve grafts and anisotropic scaffolds resulted in better functional outcome compared to isotropic scaffolds as measured by the relative gastrocnemius muscle weight (RGMW). Additionally the state of neuromuscular junctions as assessed by pre- and post-synaptic staining revealed that both the anistropic scaffolds performed as well as nerve grafts.

1. INTRODUCTION

Injuries to peripheral nerves may occur due to trauma or surgical procedures, which can result in the loss of muscle function, impaired sensation and/or painful neuropathies. The standard technique for repair is to transplant autologous nerve grafts from uninjured sites to the injured site. Even though nerve grafts are considered as the ‘gold standard’ for nerve repair, they do not result in complete nerve regeneration and recovery [1,2]. The nerve graft also suffers from additional drawbacks, such as, sacrifice of a healthy functional tissue, an additional surgery time, and size mismatch.

*Corresponding author: Ravi V. Bellamkonda., Professor of Biomedical Engineering, Suite 3108, 313 Ferst Dr. Wallace H Coulter Department of Biomedical Engineering, Georgia Institute of Technology/Emory University, Atlanta GA 30332-0535, Email address: E-mail: ravi@bme.gatech.edu, Tel: 404-385- 5038, Fax: 404-385-5044.

To find an alternative to nerve grafts, synthetic tubular nerve guidance channels (NGCs) have been used with promising results [3–6]. Performance of the NGCs can be further enhanced by varying their properties, such as, porosity [7], electrical activity [8–10], and surface roughness [11]. Silicone NGCs promote spontaneous axonal regeneration over 10 mm nerve gaps in rats, when the distal end of NGC is sutured to the distal nerve stump. However, in almost all cases of NGC use, regeneration fails if the nerve gap is increased to 15 mm or longer [12,13]. To enhance the performance of NGCs, additional filler materials (such as hydrogels), growth factors, extracellular matrix (ECM) proteins, and fibers have been used [14–17].

ECM protein laminin (LN), present in the basement membrane of most cells, is a potent stimulator of neurite outgrowth in neurons from peripheral and central nervous systems. Also, LN enhances attachment and survival of neuronal cells [18–21]. Nerve growth factor (NGF) is a neurotrophic factor produced by the target organs of sympathetic and sensory nerves [22]. NGF has been shown to stimulate neurite outgrowth and promote the survival of sensory ganglia, including those which give rise to spinal sensory nerves and sciatic nerves [23–25]. Due to their potent functions, LN-1 (an isoform of LN) and NGF have been used successfully for neurite extension *in vitro* and for nerve regeneration *in vivo* [26–30]. Hence, in this study we have used LN-1 and NGF to promote sciatic nerve regeneration across a 20 mm nerve gap in rats.

Various hydrogel scaffolds have been used for neuronal cell culture *in vitro* and for axonal regeneration *in vivo* [31–33]. In this study we have used agarose hydrogels to promote axonal regeneration. Agarose is a polysaccharide derived from red algae. In vitro, SeaPrep® agarose hydrogel has been shown to support neurite extension from a variety of neurons in a non-immunogenic manner [34–37]. Various proteins and glycosaminoglycans can be covalently linked to the agarose gels through functional groups on its polysaccharide chains. For example, LN-1 protein or fragments of LN-1 can be covalently coupled to SeaPrep® agarose gels to further enhance their ability to support neurite extension [30]. Photochemical conjugation can be used to photoimmobilize gradients of LN-1 in agarose gels to promote enhanced neurite extension *in vitro* [38].

Neurotrophic factors, such as NGF, used to promote nerve regeneration have short half-lives, and regeneration over long nerve gaps occurs over a period of weeks, therefore the use of slow release delivery vehicles is important. For slow-release of various molecules, such as growth factors and plasmid DNA phosphatidyl choline based lipid microtubules (LMTs) have been developed [39–41]. The LMTs are ideal for such sensitive molecules because they can be loaded into the LMTs in an aqueous environment without exposure to organic solvents. LMTs can also be easily embedded in agarose scaffolds facilitating slow-release of trophic factors, without physically impeding the growth cones that navigate the scaffolds. By controlling the amount of protein loaded into the microtubules, the number of microtubules used, and the length of microtubules; it is possible to control the duration of release of protein and the amount of protein released [42]. In this study we have used LMTs for slow-release of NGF, and by loading different amounts of LMTs in different parts of the scaffold; we created NGF gradients to promote axonal regeneration.

Polymer guidance channels with uniform distribution (*isotropic*) of LN-1 and NGF promote nerve regeneration comparable to that of nerve autografts over 10 mm nerve gaps in rodents [43]. However, we hypothesized that for longer nerve gaps, 15-mm or more in rodents or over 80 mm in humans, *isotropic* scaffolds might not be able to match the performance of nerve autogratfts. *Anisotropic* agarose hydrogel scaffolds, with gradients of LN-1, have been shown to promote enhanced neurite extension from chick dorsal root ganglia (DRG) *in vitro*, as compared to *isotropic* scaffolds [38]. Similarly, gradients of NGF can initiate turning of neurites towards the NGF-source [44], and guide the neurite growth [28,45]. We hypothesized

that *anisotropic* scaffolds with gradients of both LN-1 and NGF will promote enhanced axonal regeneration and better functional outcome than *isotropic* scaffolds over long nerve gaps. Here, we describe the design and fabrication of *anisotropic* scaffolds containing gradients of LN-1 and NGF to bridge a challenging 20 mm nerve gap in rats, and compare anatomical and functional outcomes as compared to the clinical gold standard of nerve grafts as well as isotropic scaffolds with uniformly distributed LN-1 and NGF.

2. MATERIALS AND METHODS

2.1. Design of the Anisotropic and Isotropic Scaffolds

2.1.1. Preparation of the Polysulfone Nerve Guidance Channels—Tubular Polysulfone NGCs (Koch Membrane System, Ann Arbor, MI) were used as carriers of LN-1 and NGF-containing agarose hydrogel scaffolds for sciatic nerve regeneration in rats. Polysulfone NGCs had an inner diameter of 1.6 mm, an outer diameter of 3.2 mm, and length of 22 mm. Before filling the NGCs with the agarose scaffold, they were sterilized by immersion in 70% ethanol solution for 1 day, dried under a clean laminar flow hood, and washed with sterilized Phosphate Buffered Saline (PBS) (Mediatech Inc., Herndon, VA). The NGCs were kept hydrated in 0.1M PBS (pH 7.4) until they were filled with the agarose scaffolds.

2.1.2. Fabrication of LN-1 coupled Agarose Hydrogels and LMTs for the Slow Release of NGF—The agarose hydrogel scaffolds were designed with three components: 0.5% (w/v) agarose hydrogel, immobilized LN-1, and NGF-loaded microtubules; for spatially and temporally controlled presentation of ECM and trophic factors *in vivo.* First, thermo-reversible SeaPrep® agarose hydrogel (BMA, Rockland, Rockland, ME) was covalently coupled with ECM protein LN-1 using photochemical conjugation technique reported previously [38]. Briefly, LN-1 (BD Biosciences, Bedford, MA) was first conjugated to a bi-functional photochemical crosslinker, Sulfo-SANPAH (Sulfosuccinimidyl-6-[4′-azido-2′-nitrophenylamino] hexanoate) (PIERCE, Rockford, IL) through the amine groups on the LN-1 molecule. An agarose solution was then added to this LN-1 – Sulfo-SANPAH conjugate such that final concentration of agarose was 1% (w/v). The solution mixture was then exposed to ultra-violet light, binding LN-1 to agarose through the photocrosslinker. The solution was then solidified into a gel by cooling in a refrigerator at 4°C for 20 minutes. Over the next 2 days, the gel was washed using 1X PBS, with repeated changes, to remove uncoupled LN-1 molecules. The LN-1 conjugated agarose hydrogel was then liquefied by heating at 45°C, and cooled to room temperature. Amount of LN-1 conjugated to agarose hydrogel was quantified by Bradford protein assay (BIO-RAD, Hercules, CA). The LN-1 –agarose solution was then mixed with equal volume of NGF-loaded microtubules and injected into polymer guidance channels in liquid state, followed by cooling for 20 min at 4° C, causing the gels in the NGCs. Preparation of NGF-loaded LMTs is describedb below.

2.1.3. NGF release from NGF-loaded LMTs—A drug delivery system using LMTs of 1,2-bis (tricosa-10,12-diyomoyl)-sn-3-phosphocholine (DC8,9PC; Avanti Polar Lipids, Inc., Alabster, AL) was prepared by ethanol deposition method, and used for slow-release of NGF, as described in other studies [30,42]. The LMTs had an average length of 45±20 μm (Figure 1). NGF is slowly released by diffusion from the two open ends of the LMTs.

A study was designed to assess the long-term release of NGF from LMTs. Lyophilized LMTs (10 mg) was rehydrated with NGF solution (0.4 ml of 120 μg/ml solution), overnight at 4°C. The solution was then centrifuged to precipitate LMTs, and the supernatant containing free NGF was removed. The LMTs were mixed with equal volume of 2% agarose solution (w/v) to form a 1% (w/v) LMT-embedded agarose solution. A volume of 300 μl of the mixture was added to a 24 well-plate dish (Corning Inc., Corning, NY) and cooled in refrigerator (4°C) for

20 minutes, to allow it to solidify. About 500 μl of PBS was added on top of the gel block, and the 24 well-plate dish was maintained at 37°C for the duration of the study. NGF, slowly released from the two open ends of LMTs, diffused into the PBS solution. The PBS solution was replaced with fresh PBS daily, and the amount of NGF in the supernatant was quantified using NGF ELISA kit (Chemicon International, Temecula, CA) to determine the amount and duration of NGF released from the LMTs.

2.1.4. Synthesis of Isotropic Scaffolds—Isotropic scaffolds with uniform distribution of LN-1 and NGF within the hydrogel scaffolds were designed. LN-1 conjugated agarose solution (66 μg of LN-1/ml of 1% agarose) was synthesized as described above, and mixed with equal volume of NGF-loaded LMTs in PBS solution (9.6×10^8 LMTs/ml of PBS, loaded with 120 μg/ml of NGF). This resulted in 0.5% agarose solution with LN-1 (33 μg/ml) and NGF-loaded LMTs (4.8×10^8 LMTs/ml). The agarose solution mixture was then injected into 22 mm long Polysulfone NGCs using a 1 ml syringe fitted with 22G needles (Becton Dickinson & Co., Franklin Lakes, NJ) and gelled by cooling at 4°C for 20 minutes. These scaffolds were kept hydrated in 0.1M PBS until implantation in rats, on the same day.

2.1.5. Synthesis of Step-gradient Anisotropic Scaffolds—Two kinds of anisotropic scaffolds were designed, one with step-gradients, and the other with continuous-gradients of LN-1. Both, step-gradient and continuous-gradient scaffolds had four layers of gels from one end of the tube to the other, each with higher concentration of NGF than the previous layer when going from proximal to distal end. However, in a step-gradient scaffold the LN-1 concentration increased in step-wise manner from one layer to another (Figure 2), whereas, in a continuous-gradient scaffold the LN-1 concentration increased smoothly from one end of tube to the other end (Figure 3).

Agarose solution (0.5% w/v) with immobilized LN-1 (33 μg/ml) and mixed in NGF-loaded LMTs (called solution 4) was prepared as described above. Solution 4 was then diluted with 0.5% agarose solution to form solution 3 with lower concentration of LN-1 (25 μg/ml) and NGF-loaded LMTs (3.6×10^8 LMTs/ml). Similarly, solution 2 (16.5 μg/ml LN-1 and 2.45×10^8 LMTs/ml) & solution 1 (8.25 μg/ml LN-1 and 1.23×10^8 LMTs/ml) were made. Solution 4 was first injected into the polymer guidance channel to fill 25% of volume and allowed to gel by cooling at 4°C for 10 minutes. The solutions 3, 2 and 1, were then injected into the polymer guidance channel, one after the other, to make four layers of gels. The four layers resulted in increasing concentrations of LN-1 and NGF from one end of tube to the other end. Figure 2A shows schematic of a step-gradient NGC connected to the two nerve ends. The LN-1 and NGF-loaded LMTs distribution in a step-gradient scaffolds are also shown (Figure 2B and 2C).

2.1.6. Synthesis of Continuous-gradient Anisotropic Scaffolds—To design anisotropic scaffolds with continuous-gradients of LN-1 and NGF, first a step-gradient of NGF-loaded LMTs was synthesized and a LN-1 gradient was made later. A 0.5% agarose solution mixture (solution 4) was first made by mixing 1% agarose solution (no LN-1) with equal volume of NGF-loaded LMTs (resulting in 4.8×10^8 LMTs/ml of PBS). Solution 4 was diluted with 0.5% plain agarose solution to make Solution 3 (3.6×10^8 LMTs/ml). Similarly, solution 2 (2.45×10^8 LMTs/ml) & solution 1 (1.23×10^8 LMTs/ml) were prepared. Solution 4 was first injected into the 22 mm long polymer guidance channel to fill 25% of volume, and allowed to gel by cooling. The solutions 3, 2 and 1 were then injected into the polymer NGCs, sequentially; to make four layers of gels, with increasing concentrations of NGF-loaded LMTs (no LN-1). A LN-1 gradient was then made by allowing controlled diffusion of LN-1-sulfo-SANPAH solution (0.68 μg/ml of LN-1) into the guidance channel through one of its end for 20 hrs (justification for 20 hrs is provided in the results, section 3.1). The LN-1 gradient was then immobilized by UV-photocrosslinking. Figure 3A shows a schematic of a continuous

gradient NGC connected to the nerve ends. The actual distribution of LN-1 and NGF-loaded LMTs is also shown (Figure 3B and 3C). To make *anisotropic* scaffolds with gradient of LN-1 but uniform NGF concentration, first, the entire NGC was filled with solution 4, and then a diffusion gradient of LN-1 was made.

To determine the concentration profile of LN-1 in continuous-gradient scaffolds, the tubes were cut transversely into 4 parts, 5-mm each. The total amount of LN-1 in each section was determined by LN-1 ELISA.

2.1.7. Experimental Groups for in vivo experiments—Nerve implants were separated into 10 groups depending on their constituents, as described in Table 1. Control group I (Saline) contained PBS solution. Control group II (Plain agarose) contained 0.5% agarose solution without any LN-1 or NGF. Control group II (LN(U)) contained LN-1-coupled 0.5% agarose gel (33 μg/ml of LN-1 uniformly distributed in the gel volume). Control group IV (nerve graft) consisted of 20 mm long nerve grafts harvested from isogenic Fischer inbred rats. Experimental group I (LN(U)-NGF(U)) contained uniform concentration of LN-1 and NGF. Experimental group II (LN(U)-NGF(SG)) contained uniform concentration of LN-1 and step-gradient of NGF. Experimental group III (LN(SG)-NGF(U)) contained step-gradient of LN-1 and uniform concentration of NGF. Experimental group IV (LN(SG)-NGF(SG)) contained step-gradient of both LN-1 and NGF. Experimental group V (LN(CG)-NGF(U)) contained continuous-gradient of LN-1 and uniform concentration of NGF. Experimental group VI (LN(CG)-NGF(SG)) contained continuous-gradient of LN-1 and step-gradient of NGF. After preparation, these implants were stored at 4°C in PBS until implantation *in vivo*, on the same day.

2.2. *In Vivo* Implantation of NGCs

A sciatic nerve transection injury model in rats was used. Adult Fischer inbred male rats (Harlan), weighing between 300–350g, were used. The rats were anesthetized using inhaled isofluorane gas (3–4% v/v for induction, 1.5–2% for maintenance, Airco, Inc., Madison, Wis.). The right thigh region was shaved and the skin was sterilized by applying chlorohexidine solution (2%, First Priority, Inc., Elgin, IL) and 70% ethanol, alternatively, 2–3 times. A 25 mm long skin incision was made along the femoral axis. The thigh muscles were separated and the sciatic nerve was dissected free. Using micro-scissors, the nerve was transected and a 5 mm nerve segment was explanted. The proximal and distal nerve stumps were secured 20 mm apart in a 22 mm long polymer guidance channel containing the experimental or control gel formulations, using a 10-0 Nylon monofilament suture (Ethicon Inc., Somerville, NJ). In case of the positive control group, the nerve gap was bridged using a 20 mm long syngenic nerve graft obtained from another Fischer inbred rat. The standard procedure of using nerve graft from the same rat could not be used, because cutting a 20 mm long nerve section and suturing it back created tension at the suture lines. The muscles were then closed using a 4-0 vicryl suture (Ethicon Inc., Somerville, NJ) and the skin was closed using wound clips (Braintree Scientific, Inc., Braintree, MA). Marcaine (0.25% w/v, Hospira, Inc., Lake Forest, IL) was administered subcutaneously for pain relief (0.2 ml/rat). The explanted 5 mm nerve was fixed in para-formaldehyde and prepared for histological analysis to evaluate the native nerve prior to injury. After surgery the rats were housed separately with access to food and water ad libitum in a colony room maintained at constant temperature (19–22°C) and humidity (40–50%) on a 12:12 h light/dark cycle. Animals were maintained in facilities approved by the Institutional Animal Care and Use Committee (IACUC) in accordance with the current United States Department of Agriculture, Department of Health and Human Services, and National Institutes of Health regulations and standards.

In case of *anisotropic* scaffolds the tubes were sutured to the nerve such that the concentration of LN-1 and NGF-releasing LMTs increases from the proximal end to the distal end. The rats were under observation for 4-months before nerve regeneration was evaluated.

2.3. Evaluation of Nerve Regeneration

2.3.1. Histological Analysis for Nerve Regeneration—Four months post-implantation, the rats were administered an intraperitoneal overdose of anesthetic cocktail (consisting of ketamine at 65mg/kg of rat weight, xylazine at 7.5mg/kg, and acepromazine 0.5mg/kg). The rats were then perfused intracardially with saline, followed by cold 4% parafomaldehyde and 0.25% gluteraldehyde (both from Sigma-Aldrich, St. Louis, MO) in 0.1 M PBS. The site of nerve injury was opened and the implant (polymer NGC or nerve graft) was removed for histological analysis. Along with the nerve implant, the gastocnemius muscle from the right (experimental side) and left (control side) limb were also explanted. All the harvested tissues were post-fixed, overnight, in 4% parafomaldehyde.

The nerve explants were cut into three equal parts: proximal, middle and distal, and additionally post-fixed, overnight, with 1% osmium tetroxide in PBS. After washing with PBS and dehydration in graded ethanol series, the three parts were separately embedded in LX112 resin (Ladd Research Industries, Inc., Burlington, VT). Semi-thin sections (0.5 μm) of nerve explants were cut using microtome, stained with Toluidine blue (0.1%, Sigma, St. Louis, MO) and observed under a light microscope. Ultra-thin sections (100 nm) were observed under electron microscope.

Nerve regeneration was evaluated at the center (10-mm) and distal end (17-mm) of the NGC/nerve graft by: a) percentage of guidance channels with successful nerve regeneration, indicated by presence of myelinated axons, b) the total number of myelinated axons, c) the area of axonal regeneration, d) the number of myelinated axons per unit area (density); and e) the diameter distribution of regenerated axons for each group. For quantification, images were captured using Sony digital photo camera (Japan) attached to Nikon Eclipse TE 300 microscope (Japan) running ImagePro® software (Media Cybernetics, L.P., Silver Spring, MD). First, images were captured using 4x or 10x objective lenses to determine the area of axonal regeneration, and then a 100x objective lens was used to count the number of myelinated axons. In the regenerated tissue the axons were evenly distributed, and hence for analysis, the areas were selected randomly. 4–5 images (at 100x) were captured for each nerve implant, so that 15–50% of area of regeneration was used for analysis and total number of myelinated axons was computed for each implant. One-way ANOVA was used for statistical comparison of the various groups, and a p-value < 0.05 was considered as statistically significant.

2.3.2. Relative Gastrocnemius Muscle Weight Measurement—The gastrocnemius muscle is innervated by the sciatic nerve, and starts atrophying after the nerve injury. The gastrocnemius muscle (not including the Soleus muscle) from the right and the left limb were harvested after the rat was sacrificed. The gastrocnemius muscle was collected after sacrificing the rats by perfusion. In order to account for any effects on muscle weight due to perfusion, rats from control as well as experimental groups were sacrificed by perfusion. All the rats with implants, in each group, were used to calculate relative gastrocnemius muscle weight (RGMW). The RGMW, which is defined as the ratio of the weight of muscle from the experimental side to the control side, was used as one of the parameter for motor function recovery. The RGMW should increase following the sciatic nerve regeneration and successful reinnervation of the muscle.

2.3.3. Neuromuscular junction (end plates), synaptic vesicles and neurofilament staining—Gastrocnemius muscle explanted from the experimental rats were post-fixed

overnight in 4% paraformaldehyde, washed with saline solution and left overnight in 30% sucrose solution. The muscle tissue was then cryoembedded. Longitudinal sections, 25 μm thick, were cut using a Microtome (Cryo-star HM 560MV, Microm, Waldorf, Germany). The 25 μm thick sections of gastrocnemius muscles were collected every 800 μm. The mass and thickness of gastrocnemius muscle varied for different groups depending upon extent of regeneration, and hence the number of sections obtained from each rat varied. The number of sections from each rat varied from 5 (minimum) to 9 (maximum). All the sections were processed for the following markers: *neurofilament 160* (NF160, Sigma-Aldrich, St. Louis, MO), *synaptic vesicles 2 protein* (SV2, Developmental Studies Hybridoma Bank, Iowa City, IA), and *acetylcholine receptors* (using alpha-Bungarotoxin-tetramethlyrhodamine, Sigma-Aldrich, St. Louis, MO) to identify new neuromuscular synapses formed as a result of nerve regeneration.

3. RESULTS

3.1. LN-1 and NGF distribution in Isotropic and Anisotropic Scaffolds

LN-1 Concentration in Isotropic Scaffolds—Bradford assay (BIO-RAD, Hercules, CA) was used to determine the amount of LN-1 coupled to agarose gel. Efficiency of the conjugation technique was about 10–15%. Using a LN-1 solution of 0.51 mg/ml as starting solution, LN-1-agarose gel with LN-1 concentration of 66 μg/ml of 1% agarose solution could be made, and this solution was used for the *in vivo* experiments.

NGF Release Study—*In vitro* NGF-release from LMTs was followed up to 18 days (Figure 4). The cumulative amount of NGF released over the 18 days was 60 nanograms. Since this amount was released into 500 μl of PBS supernatant, the NGF concentration in the supernatant would be 120 ng/ml after 18 days. For the first 6 days, the cumulative amount of NGF released was linear and rapid, and for the next 12 days the cumulative release still increased linearly, but less rapidly. The NGF-release curve did not reach a plateau after 18 days. The amount of NGF released on 18^{th} day was still much above the detection limit for the NGF ELISA kit, indicating that NGF can be released for more than 18 days from the LMTs.

LN-1 distribution in anisotropic scaffolds—A continuous-gradient of LN-1 was made by allowing controlled diffusion of LN-1 into the anisotropic scaffolds through one end of the polysulfone tubes. By varying the duration of diffusion, different LN-1 distribution profiles were obtained. The continuous-gradient anisotropic scaffolds with LN-1 distribution close to that of step-gradient anisotropic scaffolds (4 layers of gel with 33 μg/ml, 25μg/ml, 16.5μg/ml, and 8.25 μg/ml, respectively, Figure 3B) were used for *in vivo* studies, so that their performance can be compared. To obtain such LN-1 distribution, LN-1 solution (0. 68 μg/ml) was allowed to diffuse through one end of the polysulfone tube for 20 hrs, and then immobilized by photocrosslinking.

LN-1 distribution in continuous-gradient anisotropic scaffolds was determined by LN-1 ELISA (Figure 5). The 20 mm scaffolds were cut transversely into 4 parts, 5 mm each, the LN-1-agarose gel was pipetted out, and LN-1 ELISA was performed. In figure 5, LN-1 concentration distribution is plotted along the length of NGC. The average LN-1 concentration in a 5 mm section has been plotted at mid-length (i.e. at 2.5 mm, 7.5 mm, etc.). Since, these scaffolds had LN-1 distribution close to that of step-gradient anisotropic scaffolds, they were used for *in vivo* studies, so that their performance can be compared.

3.2: Histological Analysis for Nerve Regeneration

3.2.1. Presence of Regenerating Axons in Nerve Implants—A total of 10 groups were studied and only 3 groups had axonal regeneration through the implants, as determined

by histological analysis (Table 2). The 3 groups were, rats with *nerve grafts*, *LN(SG)+NGF (SG)* (step-gradient of LN-1 and NGF), and *LN(CG)+NGF(SG)* (continuous-gradient of LN-1 and step-gradient of NGF). The success rate was highest for nerve grafts with 83.3% of the rats showing regeneration, followed by LN(SG)+NGF(SG) (44.4%) and LN(CG)+NGF(SG) (37.5%) (Table 2). Rest of the histological analysis (axonal area, number of myelinated axons, etc.) could be done for these 3 groups only.

The photographs of histology specimen of cross sections at the mid-point of nerve guidance channels/autografts/normal nerve are shown in Figure 6(A–D). The gross structure of the regenerated nerves was similar to the normal sciatic nerve. Regenerated axons were packed in bundles in thin perineurial-like sheaths to form fascicles, and several fascicles were enclosed in the connective tissues of epineurium. There were abundant blood vessels in the epineurium of regenerated nerves. The implanted agarose gels were completely resorbed without any trace. Electron microscopy of ultra-thin sections of implants revealed presence of many unmyelinated axons and large numbers of nuclei from Schwann cells clearly surrounding the myelinated axons (Figure 7). The thickness of myelin sheath around the axons is greatest for the native nerve (Figure 7A) followed by the nerve grafts (Figure 7B) and then the anisotropic scaffolds (Figure 7C and 7D). The step-gradient and continuous-gradient scaffolds have similar thickness for the myelin sheath.

3.2.2. Axonal Area of Regeneration—The area of regeneration was measured at mid-length (10-mm) and distal end (17-mm) of the implants for the 3 groups which showed nerve regeneration. At mid-length as well as the distal end, the area was significantly higher for the nerve grafts than the anisotropic scaffolds. However, there was no significant difference between the two anisotropic scaffolds, LN(SG)+NGF(SG) and LN(CG)+NGF(SG) group (Figure 8). For each of the 3 groups, there was no significant difference between the area of regeneration at mid-length (10-mm) and at distal end (17-mm).

3.2.3. Total Number of Myelinated Axons and the Density of Myelinated Axons —For each of the 3 groups with regeneration, there was no significant difference between the total number of myelinated axons at mid-length (10-mm) and at distal end (17-mm) (Figure 9). At mid-length, the total number of myelinated axons in the nerve grafts and the LN(SG) +NGF(SG) (step-gradient) implants were not significantly different. However, at mid-length, the number of myelinated axons in the LN(CG)+NGF(SG) (continuous-gradient) implants was less than that of nerve grafts. At distal end (17-mm), there was no significant difference between the 3 groups. In the anisotropic scaffolds, the higher number of myelinated axons at the distal end could be due to higher concentrations of LN-1 and NGF at this end, resulting in branching of the existing axons. The number of myelinated axons in a normal sciatic nerve has also been plotted in Figure 9. The total number of myelinated axons in the nerve grafts and the LN(SG) +NGF(SG) group is comparable to a normal sciatic nerve. However, the LN(CG)+NGF(SG) group has lower number of myelinated axons than a normal nerve.

The regenerated axons were more densely packed in the anisotropic scaffolds than the nerve grafts and a normal nerve (Figure 10). The fiber density in anisotropic scaffolds is almost twice that of nerve grafts and five times that of a normal nerve.

3.2.4. Axonal Diameter Distribution—Diameter of the regenerating axons was measured using ImagePro® software to determine their diameter distribution, at mid-length and distal end. The diameter distribution followed a bell-shaped curve (Figure 11a). The peak of the curve, i.e., the maximum number of axons, was in the 1–2 μm diameter range for the nerve grafts as well as the anisotropic scaffolds. However, the axon-diameter distribution in a normal nerve was a bell-shaped curve with a much wider spread. In a normal nerve the maximum number of axons had a diameter range from 2–5 μm. The axon diameter distribution pattern

at distal end (17-mm) was similar to that at mid-length (10-mm) (Figure 11b). The nerve implants have more regenerated axons in the smaller diameter range than a normal nerve, and lesser axons in the larger diameter range than a normal nerve.

3.3. Relative Gastrocnemius Muscle Weight (RGMW)

The gastrocnemius muscle starts to atrophy after sciatic nerve injury, and hence, its mass is directly proportional to the extent of sciatic nerve re-innervation. There was no significant difference in RGMW values between LN(SG)+NGF(SG) (step-gradients) and nerve grafts (Figure 12). Rest of the groups had significantly lower RGMW values. Although, LN(CG) +NGF(SG) (continuous-gradient) group showed RGMW values close to that of nerve grafts, it was still significantly lower. The step-gradient scaffolds resulted in better functional outcome than continuous-gradient scaffolds. It is possible that the LN-1 and NGF concentrations in the step-gradient scaffolds are more optimal than in the continuous gradient scaffolds, resulting in higher number of myelinated axons (Figure 9) and higher RGMW (Figure 12).

3.4. Neuromuscular junction, synaptic vesicles and neurofilament staining

25 μm thick sections of gastrocnemius muscle from normal (uninjured) rats, and treatment groups (nerve graft, anisotropic and isotropic scaffolds) were stained for acetylcholine receptors (neuromuscular junctions, NMJ), neurofilament and synaptic vesiscles. NMJ (red, Figure 13) which were positive for neurofilament staining (green, Figure 13) and/or synaptic vesicles (green, Figure 13) were counted and compared for the various groups. In normal rats, 96.4% of the NMJs were positive for both pre- and post-synaptic structures. However, in the nerve grafts and the anisotropic scaffolds, only about 15% of the NMJs were positive for both pre- and post-synaptic structures. There was no significance difference in the number of NMJs between the anisotropic scaffolds and the nerve graft. In case of isotropic scaffolds, there were no NMJs that were positive for both pre- and post-synaptic structures, indicating lack of formation of new NMJs.

4. DISCUSSION

During embryonic development of the nervous system, the developing axons use a variety of haptotactic and chemotactic cues to find their target organs [46]. Some of these cues are presented in a gradient fashion in order to direct the axons towards their target tissues [47, 48]. ECM proteins, such as laminin and fibronectin, and neurotrophic factors, such as NGF and BDNF, have been used in several studies to promote nerve regeneration *in vivo* [5,26, 49]. However, these neuro-stimulatory molecules have not been presented in a gradient fashion as observed *in vivo*. To mimic *in vivo* conditions for axonal guidance and regeneration, we designed novel anisotropic scaffolds with gradients of ECM proteins and neurotrophic factors for nerve regeneration *in vivo*. Here we show that anisotropic agarose gel scaffolds with gradients of LN-1 and NGF promote enhanced axonal regeneration, as compared to isotropic scaffolds with uniform concentrations of LN-1 and NGF, across a challenging 20 mm nerve gap in rats. In this injury model, axonal regeneration is limited and does not occur unless the nerve guidance channels have gradients of both LN-1 and NGF (step- or continuous-). Scaffolds with gradient of either LN-1 or NGF, with the other component at uniform distribution, did not promote axonal regeneration across the challenging 20 mm nerve gap.

LN-1 is an appropriate candidate as the protein of choice to promote PNS regeneration since it has been shown to be a potent stimulator of neurite outgrowth [21,27,50]. In most neuronal tissues, development of the axons and formation of new synapses is preceded by migration of the neuronal cell bodies to the appropriate regions of the brain. It has been proposed that LN facilitates all of these processes in several neural systems [51–53]. The spatio-temporally controlled expression of LN-1 in the developing peripheral nervous system, as well as the visual

pathway and the cerebellum, suggests that LN plays a role in axon outgrowth and guidance [54–56]. The LN expression has been found to be essential for ventral turning of axons during development. Blocking the nidogen-binding motifs on LN prevents turning of axons, although it does not affect growth [48], indicating that LN might play a role in orientation of axons in some systems. NGF has been shown to stimulate and promote the survival of sensory ganglia [23,24]. Griffin et al. [57] have shown concentration-dependent neurite extension/retraction with NGF levels. NGF has been shown to prevent the complete death of axotomized sensory neurons following exogenous administration [58]. There is enough evidence to show that gradients of neurotrophins help in guiding developing as well as regenerating axons in a wide variety of neuronal systems [59,60]. Although many *in vitro* studies have shown influence of gradients of LN-1 and NGF for neurite extension, to our knowledge, there are no *in vivo* studies with gradients, due to the difficulties in making and sustaining gradients *in vivo*.

In this study, we present a diffusion technique to first make gradients of LN-1 in agarose gel and then immobilize it using photochemical cross-linking. Immobilization of LN-1 imitates *in vivo* conditions where LN-1 is tethered to ECM. Gradients of NGF were designed using slow-release LMTs, which imitates *in vivo* conditions where neurotrophins are released by target organs and taken up by nerve ends. Two kinds of LN-1 gradients were designed, a step-gradient and the other a continuous-gradient, to promote nerve regeneration. However, the NGF gradient was always a continuous-gradient due to the diffusion of NGF. The step- and continuous-gradient scaffolds of LN-1 were designed such that the average LN-1 concentration in both conditions is very close. However, the actual concentration of LN-1 that the regenerating axons will sense dynamically in each condition will be different because of the difference in gradient profile. For example, in step-gradients, from 0–5 mm distance, axons will see uniform concentration of LN-1 (8.25 μg/ml), whereas, in a continuous-gradient, axons will see increasing concentration profile of LN-1, but with an average LN-1 concentration of 5.1 μg/ml. The LN-1 concentration range selected for making LN-1 step-gradients was based on the maximum concentration of LN-1 that could be immobilized. However, this concentration range may not be the optimal range. A more thorough study will be needed to determine the optimal LN-1 concentration range for nerve regeneration.

Nerve regeneration over a 20 mm nerve gap in rats is challenging, and the failure of axonal regeneration in 7 out of the 10 experimental groups is a testament to the degree of difficulty of this model. Nerve regeneration was observed only when the scaffolds had gradients of both LN-1 and NGF. Scaffolds with gradient of only LN-1 or only NGF, with the other component at uniform concentration, were not able to promote nerve regeneration. This suggests a synergistic effect between LN-1 and NGF, as mentioned in a previous study [43]. Also, it suggests that while scaffolds with uniformly distributed LN-1 and NGF matched the performance of nerve autografts in our previous studies while bridging 10 mm nerve gaps, it is very important to test longer nerve gaps as these might be more representative of those occurring in patients who might be candidates for such a procedure.

In the relative gastrocnemius muscle weight study, the anisotropic scaffolds with step-gradients of LN-1 were able to match the autografts for RGMW. Rest of the groups had significantly lower RGMW. Lower RGMW outcome with the continuous-gradient scaffolds, as compared to the step-gradient scaffolds, could be due to non-optimal concentration range of LN-1 in the continuous-gradient scaffolds. Even though both groups, nerve grafts and step-gradient scaffolds, show significant improvement in RGMW, they were still lower than the native, well-innervated muscle. It is possible that the regenerating axons take longer than 4-months to traverse the 20 mm nerve gap and the distal nerve stump, to form new neuromuscular junctions and cause muscle regeneration. A study with longer duration of regeneration may result in higher values of RGMW for both groups.

To determine formation of new neuromuscular junctions (NMJs), gastrocnemius muscle sections were stained for pre-synaptic structures (synaptic vesicles and neurofilament) and post-synaptic structure (acetylcholine receptors). In normal rats, 96.4% of post-synaptic structures were also positive for staining of pre-synaptic structures. However, in the nerve grafts and the anisotropic scaffolds, only about 15% of the NMJs were positive for both pre- and post-synaptic structures. In the implant groups, apart from the neurofilaments making synapses at NMJs, additional neurofilament staining was also observed. It was not possible to determine if these are sensory axons or motor axons, and if these would lead to formation of more NMJs in the future. Although there is no significance difference in % of NMJs staining between the nerve grafts and the anisotropic scaffolds, the total number of positive NMJs is lower with LN(CG)+NGF(SG) scaffolds than nerve grafts and LN(SG)+NGF(SG). This could be the reason that the RGMW of LN(CG)+NGF(SG) is lower than that of the nerve grafts and LN(SG)+NGF(SG).

5. CONCLUSIONS

In conclusion, we report the novel design, implementation and evaluation of anisotropic hydrogel scaffolds with embedded gradients of ECM proteins and neurotrophic factors for directed peripheral nerve regeneration. Our data demonstrates that nerve regeneration across a challenging 20-mm nerve gap occurs only when gradients of both LN-1 and NGF are present, but not when these proteins are presented in an isotropically distributed manner. However, while the step-gradient anisotropic scaffolds elicited axonal regeneration and RGMW comparable to that observed with the clinical gold standard nerve autografts, the continuous-gradient scaffolds were unable to match the performance of autografts. This suggests that more careful optimization of ECM and trophic factor gradients, their concentrations and slopes, maybe necessary to fully realize the promise of anisotropic scaffolds such that they match the performance of nerve grafts in bridging long peripheral nerve gaps. Nevertheless, our data leads one to unequivocally conclude that anisotropic distribution of trophic and ECM proteins in 3D hydrogels represents a significant step forward in the design of tissue engineered nerve bridges compared to isotropic 3D scaffolds where growth promoting proteins are uniformly distributed with no embedded directional cues.

Acknowledgements

The authors are grateful to Dr. Arthur W. English and Dr. Gail Schwartz for their skilled assistance during the immunohistochemical procedures particularly with the characterization of neuro-muscular junctions. The authors also thank Dr. Young-tae Kim, Dr. Valerie Haftel, Alex Stroh and Charmi Jani for their technical assistance. This work was supported by the National Institutes of Health (NS44409 to RVB), and the Georgia Tech/Emory Center for Engineering of Living Tissues (NSF EEC-9731643).

References

1. Meyer RS, Abrams RA, Botte MJ, Davey JP, Bodine-Fowler SC. Functional recovery following neurorrhaphy of the rat sciatic nerve by epineurial repair compared with tubulization. J Orthop Res 1997;15(5):664–9. [PubMed: 9420594]
2. Zhao Q, Dahlin LB, Kanje M, Lundborg G. Specificity of muscle reinnervation following repair of the transected sciatic nerve. A comparative study of different repair techniques in the rat. J Hand Surg [Br] 1992;17(3):257–61.
3. Aebischer P, Valentini RF, Winn SR, Galletti PM. The use of a semi-permeable tube as a guidance channel for a transected rabbit optic nerve. Prog Brain Res 1988;78:599–603. [PubMed: 3247455]
4. Ansselin AD, Fink T, Davey DF. Peripheral nerve regeneration through nerve guides seeded with adult Schwann cells. Neuropathol Appl Neurobiol 1997;23(5):387–98. [PubMed: 9364464]

5. Chen YS, Hsieh CL, Tsai CC, Chen TH, Cheng WC, Hu CL, et al. Peripheral nerve regeneration using silicone rubber chambers filled with collagen, laminin and fibronectin. Biomaterials 2000;21(15): 1541–7. [PubMed: 10885726]
6. Valentini, RF.; Aebischer, P. Strategies for the engineering of peripheral nervous tissue regeneration. In: Lanza RP, LR.; Chick, WL., editors. Principles of Tissue Engineering. Austin: R.G. Landes Company; 1997. p. 671-684.
7. Aebischer P, Guenard V, Brace S. Peripheral nerve regeneration through blind-ended semipermeable guidance channels:effect of molecular weight cutoff. J Neurosci 1989a;9:3590–3595. [PubMed: 2795143]
8. Aebischer P, Valentini RF, Dario P, Domenici C, Galletti PM. Piezoelectric guidance channels enhance regeneration in the mouse sciatic nerve after axotomy. Brain Res 1987;436(1):165–8. [PubMed: 3690349]
9. Valentini RF, Sabatini AM, Dario P, Aebischer P. Polymer electret guidance channels enhance peripheral nerve regeneration in mice. Brain Res 1989;480(1–2):300–4. [PubMed: 2713656]
10. Fine EG, Valentini RF, Bellamkonda R, Aebischer P. Improved nerve regeneration through piezoelectric vinylidenefluoride-trifluoroethylene copolymer guidance channels. Biomaterials 1991;12(8):775–80. [PubMed: 1799653]
11. Aebischer P, Guenard V, Valentini RF. The morphology of regenerating peripheral nerves is modulated by the surface microgeometry of polymeric guidance channels. Brain Res 1990;531(1–2):211–8. [PubMed: 2289122]
12. Danielsen N, Dahlin LB, Lee YF, Lundborg G. Axonal growth in mesothelial chambers. The role of the distal nerve segment. Scand J Plast Reconstr Surg 1983;17(2):119–25. [PubMed: 6658385]
13. Lundborg G, Dahlin LB, Danielsen N, Gelberman RH, Longo FM, Powell HC, et al. Nerve regeneration in silicone chambers: influence of gap length and of distal stump components. Exp Neurol 1982;76(2):361–75. [PubMed: 7095058]
14. Madison RD, Da Silva CF, Dikkes P. Entubulation repair with protein additives increases the maximum nerve gap distance successfully bridged with tubular prostheses. Brain Res 1988;447(2): 325–34. [PubMed: 3390701]
15. Matsumoto K, Ohnishi K, Kiyotani T, Sekine T, Ueda H, Nakamura T, et al. Peripheral nerve regeneration across an 80-mm gap bridged by a polyglycolic acid (PGA)-collagen tube filled with laminin-coated collagen fibers: a histological and electrophysiological evaluation of regenerated nerves. Brain Res 2000;868(2):315–28. [PubMed: 10854584]
16. Tong XJ, Hirai K, Shimada H, Mizutani Y, Izumi T, Toda N, et al. Sciatic nerve regeneration navigated by laminin-fibronectin double coated biodegradable collagen grafts in rats. Brain Res 1994;663(1): 155–62. [PubMed: 7850464]
17. English AW, Meador W, Carrasco DI. Neurotrophin-4/5 is required for the early growth of regenerating axons in peripheral nerves. Eur J Neurosci 2005;21(10):2624–34. [PubMed: 15926911]
18. Luckenbill-Edds L. Laminin and the mechanism of neuronal outgrowth. Brain Research Reviews 1997;23:1–27. [PubMed: 9063584]
19. Kleinman HK, Ogle RC, Cannon FB, Little CD, Sweeney TM, Luckenbill-Edds L. Laminin receptors for neurite formation. Proc Natl Acad Sci U S A 1988;85(4):1282–6. [PubMed: 2963341]
20. Reichardt LF, Tomaselli KJ. Extracellular matrix molecules and their receptors: functions in neural development. Annu Rev Neurosci 1991;14:531–70. [PubMed: 1851608]
21. Rivas RJ, Burmeister DW, Goldberg DJ. Rapid effects of laminin on the growth cone. Neuron 1992;8:107–115. [PubMed: 1730003]
22. Barde YA. Trophic factors and neuronal survival. Neuron 1989;2(6):1525–34. [PubMed: 2697237]
23. Levi-Montalcini R. The nerve growth factor 35 years later. Science 1987;237(4819):1154–62. [PubMed: 3306916]
24. Thoenen H, Barde YA, Davies AM, Johnson JE. Neurotrophic factors and neuronal death. Ciba Found Symp 1987;126:82–95. [PubMed: 3556091]
25. Ide C. Peripheral nerve regeneration. Neurosci Res 1996;25(2):101–21. [PubMed: 8829147]
26. Ahmed Z, Brown RA, Ljungberg C, Wiberg M, Terenghi G. Nerve growth factor enhances peripheral nerve regeneration in non-human primates. Scand J Plast Reconstr Surg Hand Surg 1999;33(4):393–401. [PubMed: 10614747]

27. Baron-van Evercooren A, Kleinman HD, Ohno S, Marangos P, Schwartz JP, Dubois-Dalcq ME. Nerv growth factor, laminin and fibronectin promote nerve growth in human fetal sensory ganglia cultures. J Neurosci Res 1982;8:179–183. [PubMed: 7154111]
28. Cao X, Shoichet MS. Investigating the synergistic effect of combined neurotrophic factor concentration gradients to guide axonal growth. Neuroscience 2003;122(2):381–9. [PubMed: 14614904]
29. Derby A, Engleman VW, Frierdich GE, Neises G, Rapp SR, Roufa DG. Nerve growth factor facilitates regeneration across nerve gaps: morphological and behavioral studies in rat sciatic nerve. Exp Neurol 1993;119(2):176–91. [PubMed: 8432358]
30. Yu X, Dillon GP, Bellamkonda RB. A laminin and nerve growth factor-laden three-dimensional scaffold for enhanced neurite extension. Tissue Eng 1999;5(4):291–304. [PubMed: 10477852]
31. Satou T, Nishida S, Hiruma S, Tanji K, Takahashi M, Fujita S, et al. A morphological study on the effects of collagen gel matrix on regeneration of severed rat sciatic nerve in silicone tubes. Acta Pathol Jpn 1986;36(2):199–208. [PubMed: 2422877]
32. Wang KK, Nemeth IR, Seckel BR, Chakalis-Haley DP, Swann DA, Kuo JW, et al. Hyaluronic acid enhances peripheral nerve regeneration in vivo. Microsurgery 1998;18(4):270–5. [PubMed: 9779641]
33. Suzuki Y, Tanihara M, Ohnishi K, Suzuki K, Endo K, Nishimura Y. Cat peripheral nerve regeneration across 50 mm gap repaired with a novel nerve guide composed of freeze-dried alginate gel. Neurosci Lett 1999;259(2):75–8. [PubMed: 10025561]
34. Strassman RJ, Letourneau PC, Wessells NK. Elongation of axons in an agar matrix that does not support cell locomotion. Exp Cell Res 1973;81(2):482–7. [PubMed: 4796638]
35. Bellamkonda RV, Ranieri JP, Bouche N, Aebischer P. Hydrogel-based three-dimensional matrix for neural cells. J Biomed Mater Res 1995;29:663–71. [PubMed: 7622552]
36. Dillon GP, Yu X, Bellamkonda RV. The polarity and magnitude of ambient charge influences three-dimensional neurite extension from DRGs. J Biomed Mater Res 2000;51(3):510–9. [PubMed: 10880096]
37. Labrador RO, Buti M, Navarro X. Peripheral nerve repair: role of agarose matrix density on functional recovery. Neuroreport 1995;6(15):2022–6. [PubMed: 8580432]
38. Dodla MC, Bellamkonda RV. Anisotropic scaffolds facilitate enhanced neurite extension in vitro. J Biomed Mater Res A 2006;78(2):213–21. [PubMed: 16892507]
39. Rudolph AS, Stilwell G, Cliff RO, Kahn B, Spargo BJ, Rollwagen F, et al. Biocompatibility of lipid microcylinders: effect on cell growth and antigen presentation in culture. Biomaterials 1992;13(15): 1085–92. [PubMed: 1493192]
40. Spargo BJ, Cliff RO, Rollwagen FM, Rudolph AS. Controlled release of transforming growth factor-beta from lipid-based microcylinders. J Microencapsul 1995;12(3):247–54. [PubMed: 7650589]
41. Meilander NJ, Pasumarthy MK, Kowalczyk TH, Cooper MJ, Bellamkonda RV. Sustained release of plasmid DNA using lipid microtubules and agarose hydrogel. J Control Release 2003;88(2):321–31. [PubMed: 12628338]
42. Meilander NJ, Yu X, Ziats NP, Bellamkonda RV. Lipid-based microtubular drug delivery vehicles. J Control Release 2001;71(1):141–52. [PubMed: 11245915]
43. Yu X, Bellamkonda RV. Tissue-engineered scaffolds are effective alternatives to autografts for bridging peripheral nerve gaps. Tissue Eng 2003;9(3):421–30. [PubMed: 12857410]
44. Gallo G, Lefcort FB, Letourneau PC. The trkA receptor mediates growth cone turning toward a localized source of nerve growth factor. J Neurosci 1997;17(14):5445–54. [PubMed: 9204927]
45. Cao X, Shoichet MS. Defining the concentration gradient of nerve growth factor for guided neurite outgrowth. Neuroscience 2001;103(3):831–40. [PubMed: 11274797]
46. Song H, Poo M. The cell biology of neuronal navigation. Nat Cell Biol 2001;3(3):E81–8. [PubMed: 11231595]
47. Bonhoeffer F, Huf J. In vitro experiments on axon guidance demonstrating an anterior-posterior gradient on the tectum. Embo J 1982;1(4):427–31. [PubMed: 6203734]
48. Bonner J, O'Connor TP. The permissive cue laminin is essential for growth cone turning in vivo. J Neurosci 2001;21(24):9782–91. [PubMed: 11739586]

49. Aebischer P, Salessiotis AN, Winn SR. Basic fibroblast growth factor released from synthetic guidance channels facilitates peripheral nerve regeneration across long nerve gaps. J Neurosci Res 1989;23(3):282–9. [PubMed: 2769793]
50. Rogers SL, Letourneau PC, Palm SL, McCarthy J, Furcht LT. Neurite extension by central and peripheral nervous system neurons in response to substratun-bound fibronectin and laminin. Dev Biol 1983;98:212–220. [PubMed: 6862106]
51. Liesi P. Do neurons in the vertebrate CNS migrate on laminin? Embo J 1985;4(5):1163–70. [PubMed: 4006911]
52. Zhou FC, Azmitia EC. Laminin directs and facilitates migration and fiber growth of transplanted serotonin and norepinephrine neurons in adult brain. Prog Brain Res 1988;78:413–26. [PubMed: 3247440]
53. Bronner-Fraser M, Stern CD, Fraser S. Analysis of neural crest cell lineage and migration. J Craniofac Genet Dev Biol 1991;11(4):214–22. [PubMed: 1725870]
54. Rogers SL, Edson KJ, Letourneau PC, McLoon SC. Distribution of laminin in the developing peripheral nervous system of the chick. Dev Biol 1986;113(2):429–35. [PubMed: 3512333]
55. McLoon SC, McLoon LK, Palm SL, Furcht LT. Transient expression of laminin in the optic nerve of the developing rat. J Neurosci 1988;8(6):1981–90. [PubMed: 3385486]
56. Liesi P, Hager G, Dodt HU, Seppala I, Zieglgansberger W. Domain-specific antibodies against the B2 chain of laminin inhibit neuronal migration in the neonatal rat cerebellum. J Neurosci Res 1995;40 (2):199–206. [PubMed: 7745613]
57. Griffin CG, Letourneau PC. Rapid retraction of neurites by sensory neurons in response to increased concentrations of nerve growth factor. J Cell Biol 1980;86(1):156–61. [PubMed: 7191423]
58. Rich KM, Luszczynski JR, Osborne PA, Johnson EM Jr. Nerve growth factor protects adult sensory neurons from cell death and atrophy caused by nerve injury. J Neurocytol 1987;16(2):261–8. [PubMed: 3625240]
59. Gundersen RW, Barrett JN. Neuronal chemotaxis: chick dorsal-root axons turn toward high concentrations of nerve growth factor. Science 1979;206(4422):1079–80. [PubMed: 493992]
60. Gundersen RW, Barrett JN. Characterization of the turning response of dorsal root neurites toward nerve growth factor. J Cell Biol 1980;87(3 Pt 1):546–54. [PubMed: 6257725]

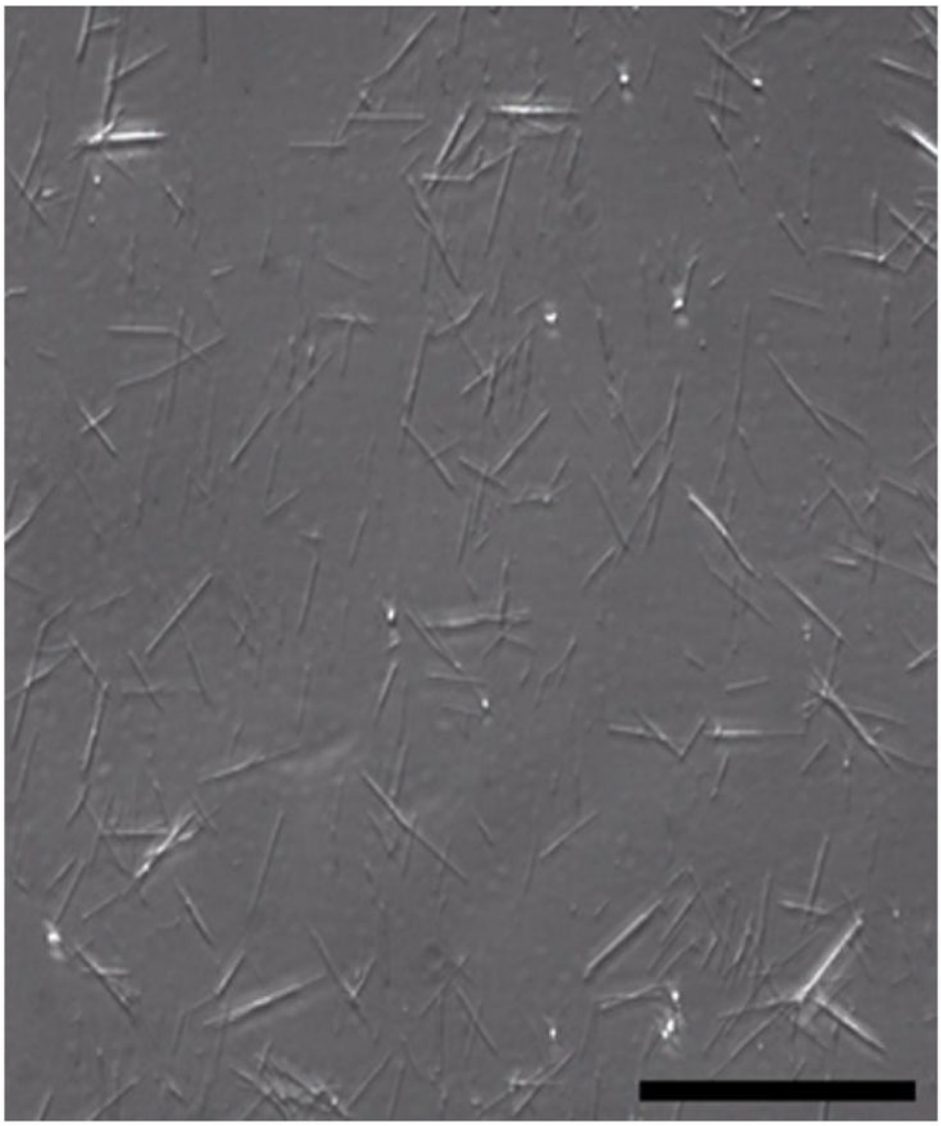

Figure 1.
Lipid microtubules. Phase- contrast image of lipid microtubules from DC8,9PC lipid. Scale bar = 100 μm.

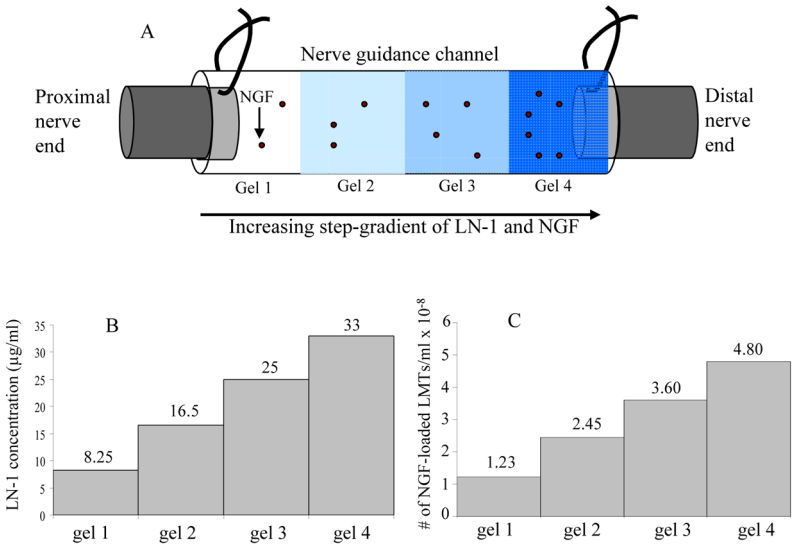

Figure 2.

LN-1 and NGF distribution in step-gradient anisotropic scaffolds. Figure 2A is a schematic of a NGC connected to nerve ends, with four layers of gels in it (A). The darker shades of gel represent increasing concentration of LN-1. Gel 4 has higher concentration of LN-1 than gel 3 and so on (Fig. 2B). Similarly gel 4 has higher concentration of NGF-loaded LMTs than gel 3 and so on (Fig. 2C). While LN-1 gradient is immobilized, with time, NGF will diffuse and form a smooth gradient.

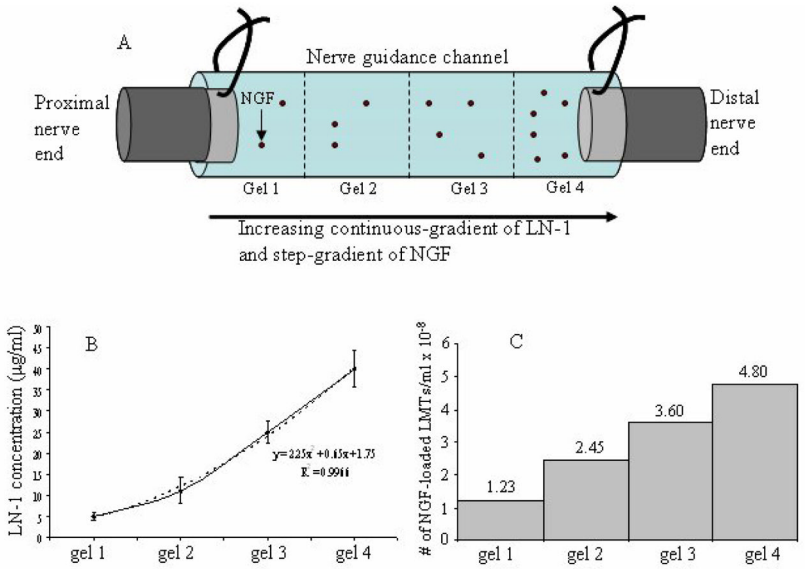

Figure 3.

LN-1 and NGF distribution in continuous-gradient anisotropic scaffolds. Figure 3A is a schematic of a NGC connected to nerve ends, with four layers of gels in it. LN-1 gradient is smooth (Fig. 3B), as determined by LN-1 ELISA, while NGF-loaded LMTs are distributed in a step-gradient fashion (Fig. 3C). With time, NGF will diffuse out of LMTs and form a smooth gradient.

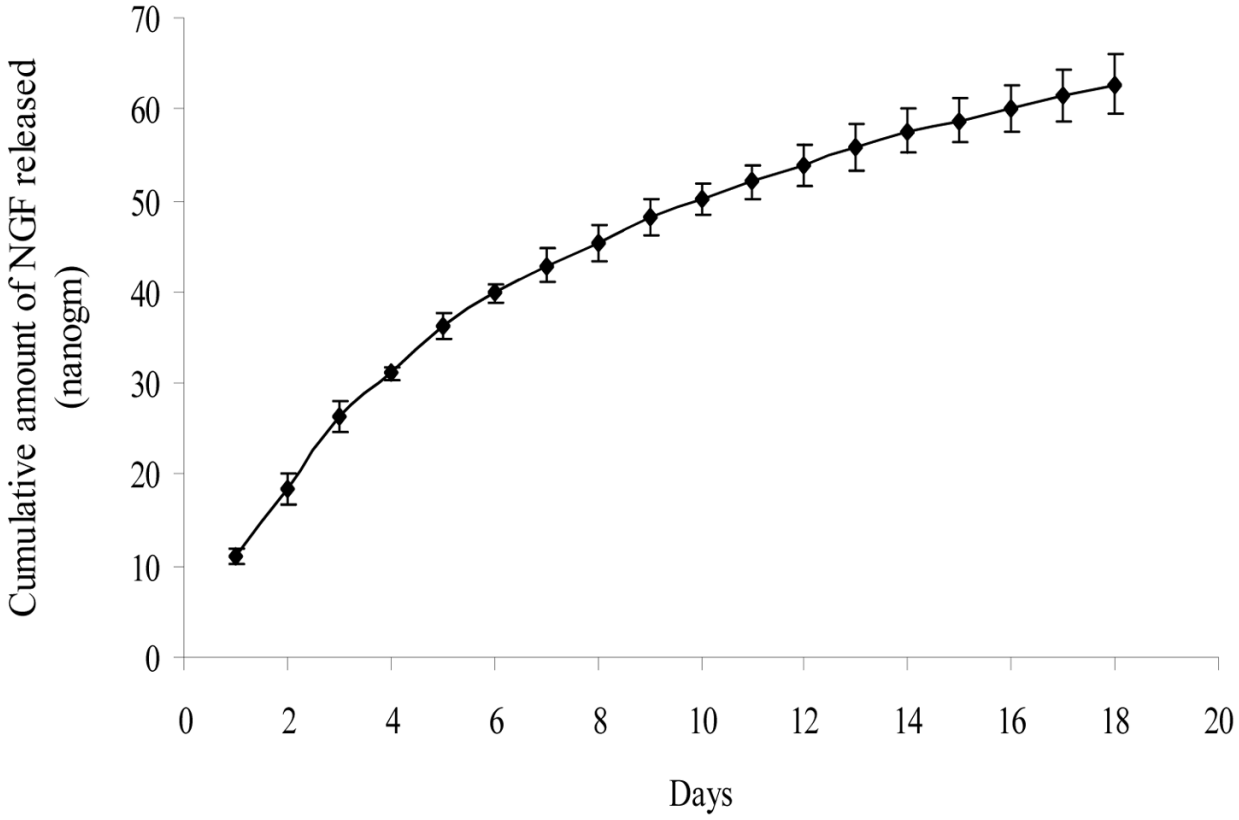

Figure 4.

NGF-release study, *in vitro*. NGF-release from LMTs was followed up to 18 days. For the first 6 days, the release profile was almost linear and rapid. For the next 12 days, the release was less rapid but still increased linearly with time. All error bars indicate standard error of mean (n = 3).

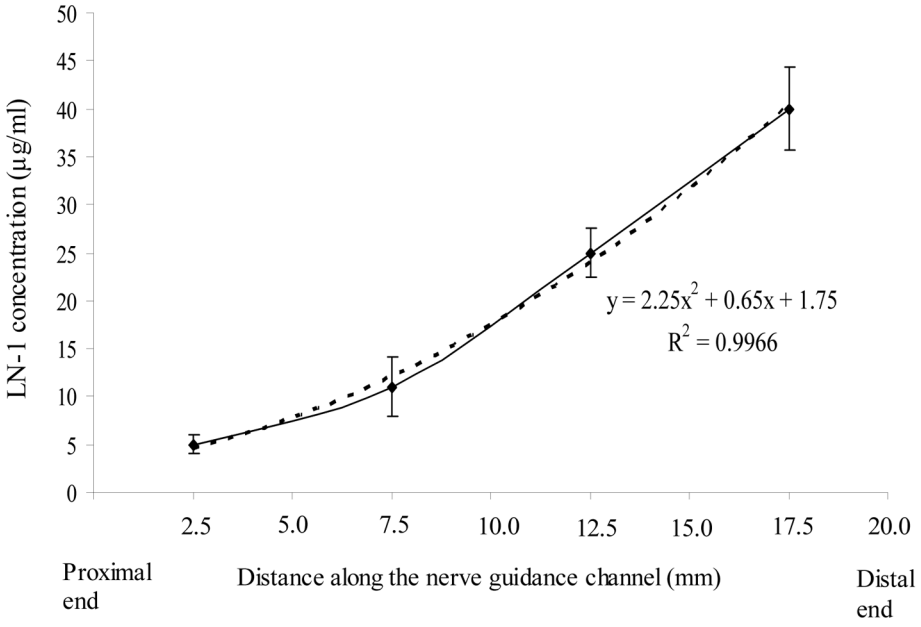

Figure 5.

LN-1 concentration distribution in continuous-gradient anisotropic scaffolds. 20-mm long nerve guidance channels with continuous-gradients of LN-1 were cut into 4 parts, each 5-mm long, and their LN-1 content was determined. The average value for each 5 mm section is plotted at mid-length. LN-1 distribution followed a second-order polynomial. All error bars indicate SEM (n = 3).

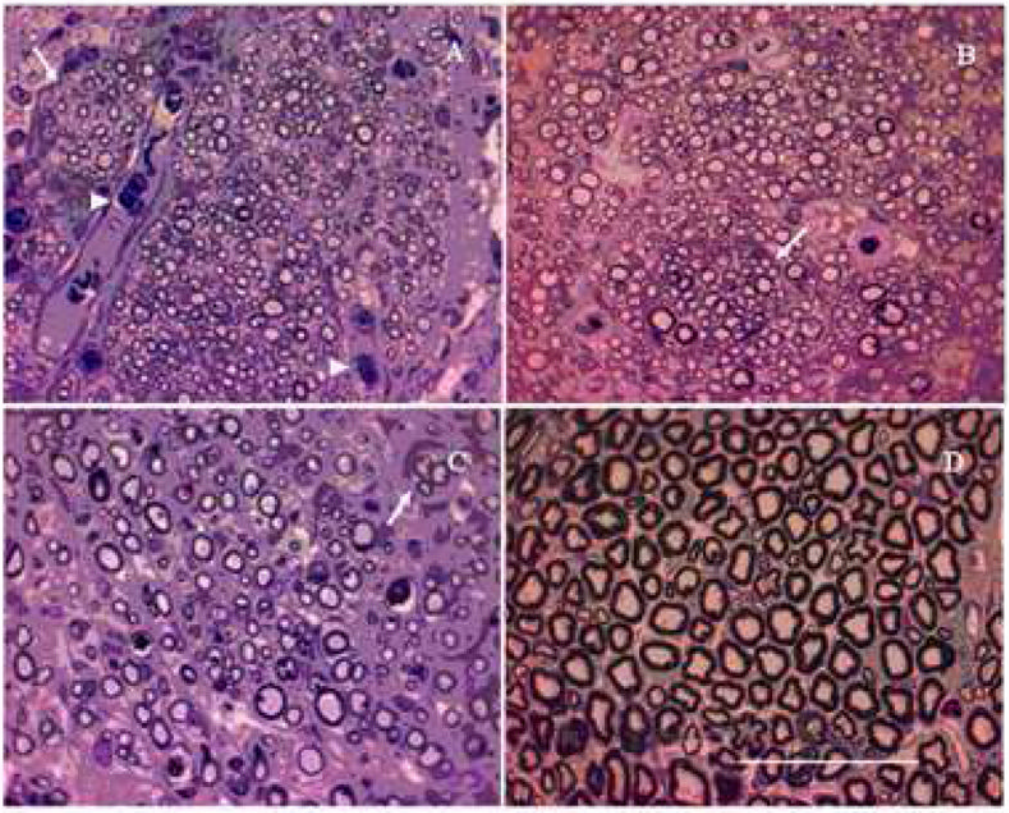

Figure 6.
Light micrographs of nerve sections from groups with successful axonal regeneration. Toludine-blue stained cross-sections at mid-length (10 mm) are shown here. Anisotropic scaffolds with step-gradient (A) and continuous-gradient (B) of LN-1, have higher density of axons and smaller-diameter axons than nerve grafts (C) and normal nerve (D). Note the fiber grouping in small fascicles (indicated by arrow) and presence of red blood cells (arrowhead). Scale bar = 50 μm

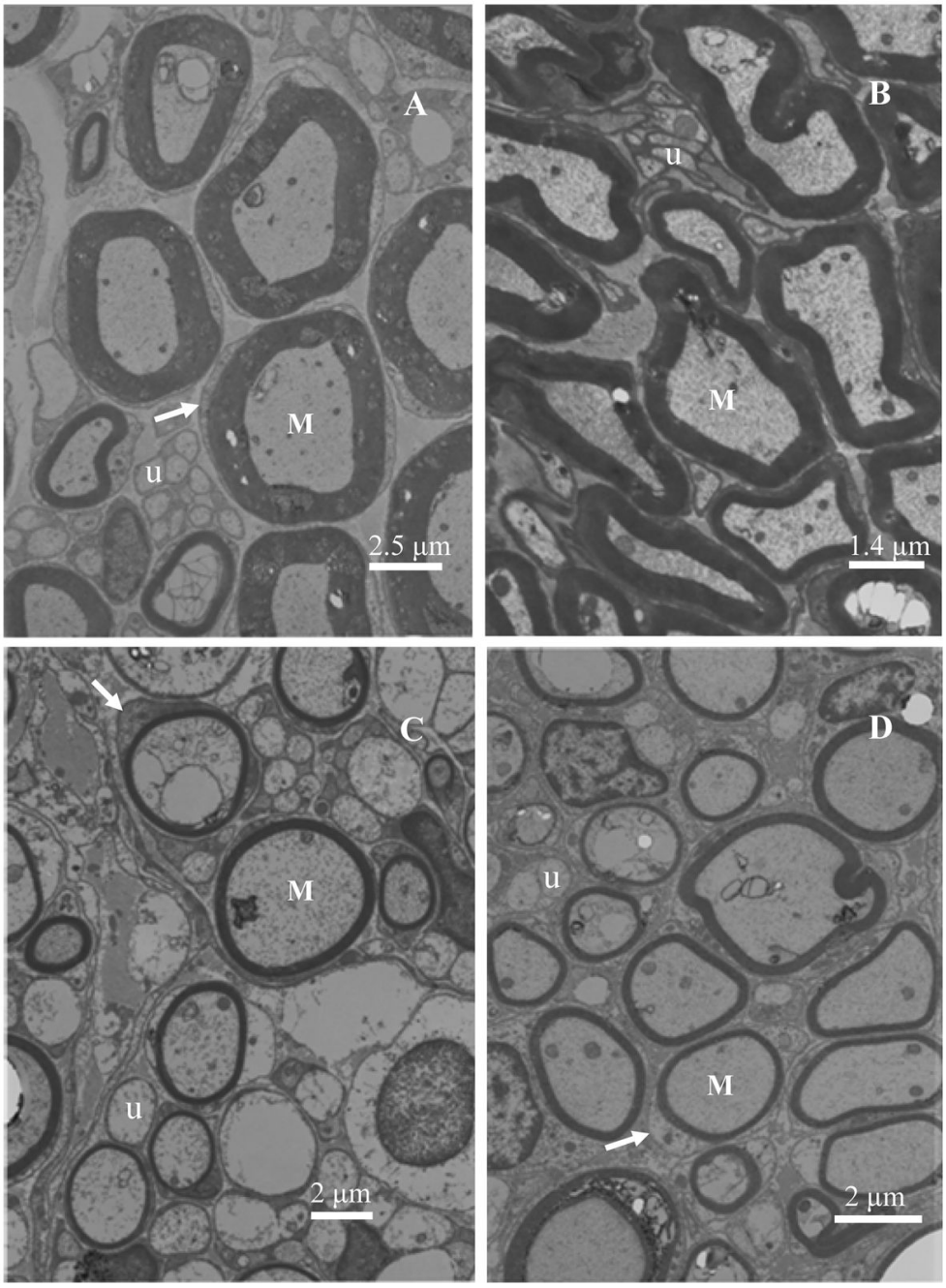

Figure 7.
Transmission electron micrographs of nerve sections at mid-length (10 mm) of implants. Myelinated axons (M), unmyelinated axons (u) and Schwann cells surrounding the myelinated axons (arrow) can be seen clearly in all four conditions. The myelin sheath thickness was greatest for the native nerve (A), followed by nerve grafts (B) and then followed by the anisotropic scaffolds (C and D).

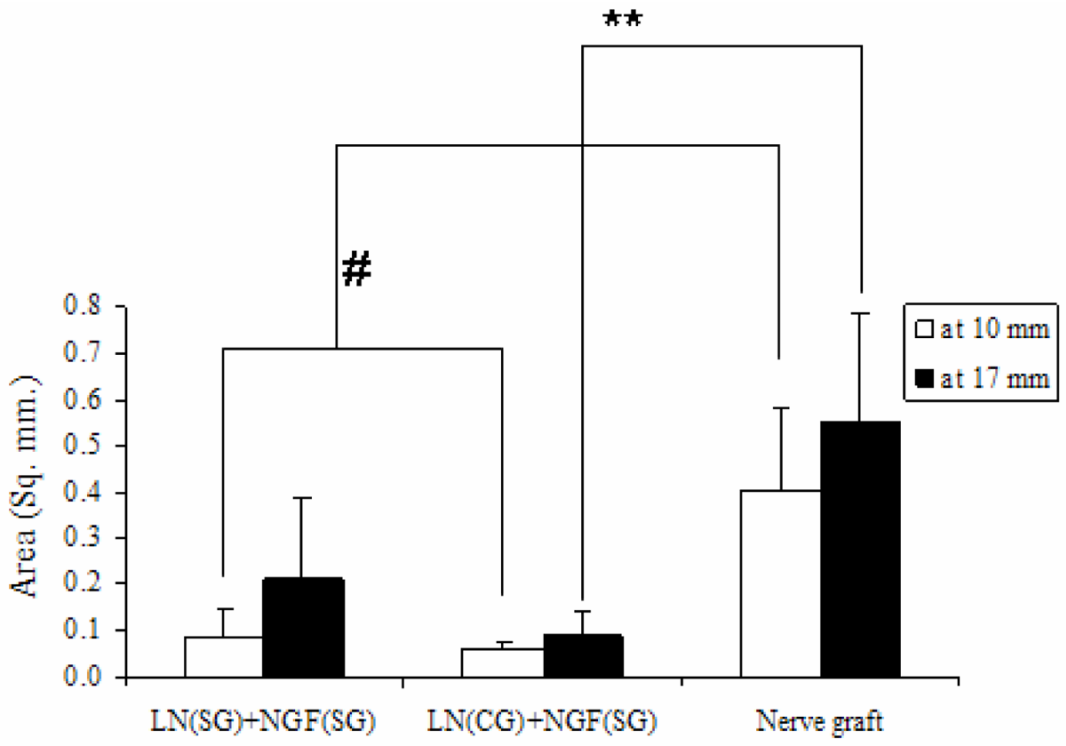

Figure 8.

Area of nerve regeneration. For all three groups, there was no significant difference between area of regeneration at distal end and at the middle. At midpoint, nerve graft has higher area of regeneration than either anisotropic scaffold group (# p-value < 0.05). However, at distal end, area in nerve graft is higher compared to continuous-gradient group only (** p-value<0.05). All error bars indicate standard error of mean.

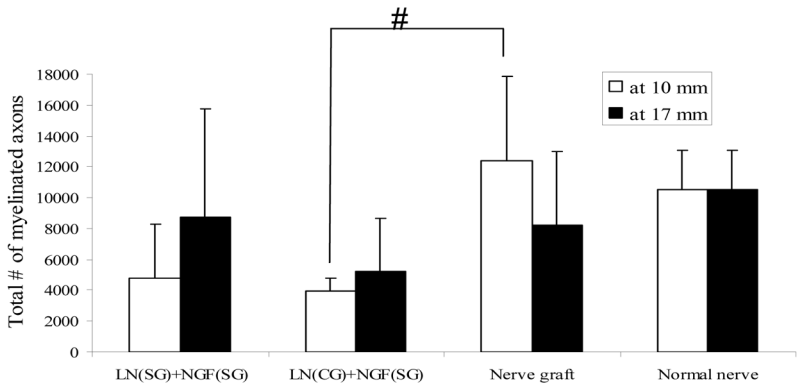

Figure 9.

Total number of myelinated axons. There was no significant difference between step-gradients and nerve grafts. There was no significant difference between the two gradient scaffolds themselves. At mid-length, the continuous-gradient scaffolds had lower number of myelinated axons than nerve grafts (# p-value < 0.05). All error bars indicate standard error of mean.

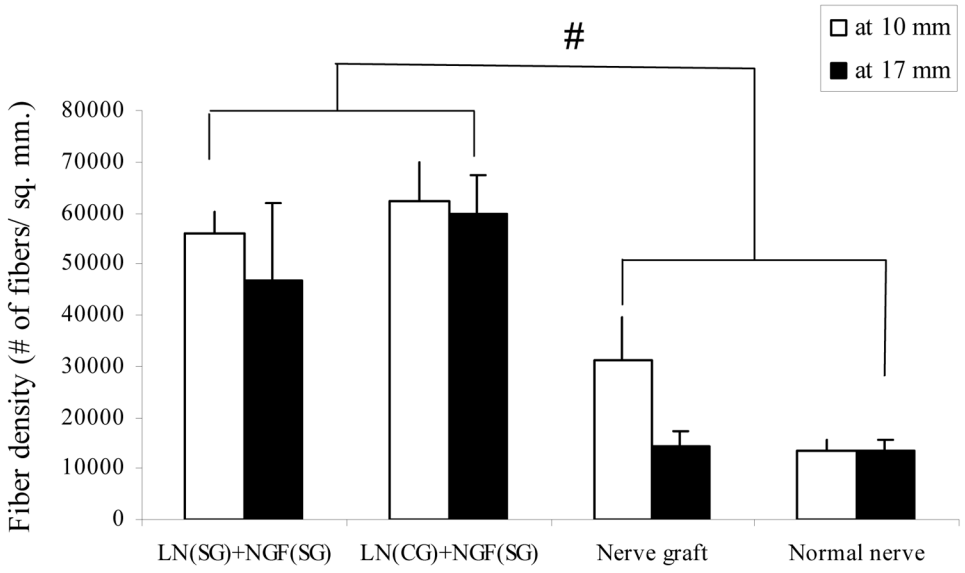

Figure 10.
Density of myelinated axons. The regenerated nerve fibers are more densely packed in anisotropic scaffolds than nerve grafts and normal nerve (# p-value<0.05). All error bars indicate standard error of mean.

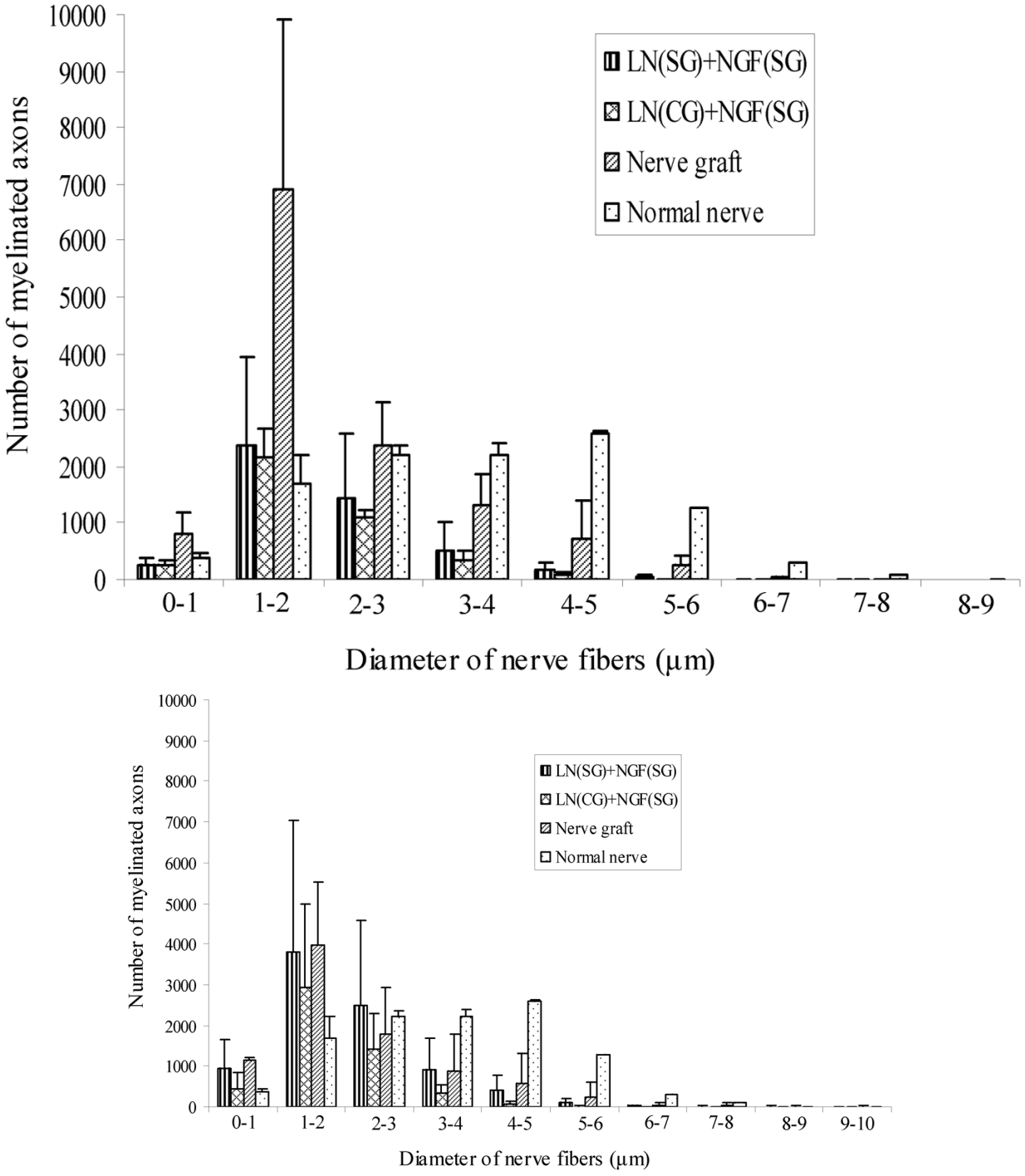

Figure 11.

Diameter distribution of nerve axons at A) mid-length (10-mm), and B) distal end (17 mm). For each group the diameter distribution is a bell-shaped curve. For all the nerve implants, the maximum numbers of axons have a diameter of 1–2 μm. However, in a normal nerve the maximum diameter distribution is broader, from 1–5 μm. All error bars indicate SEM.

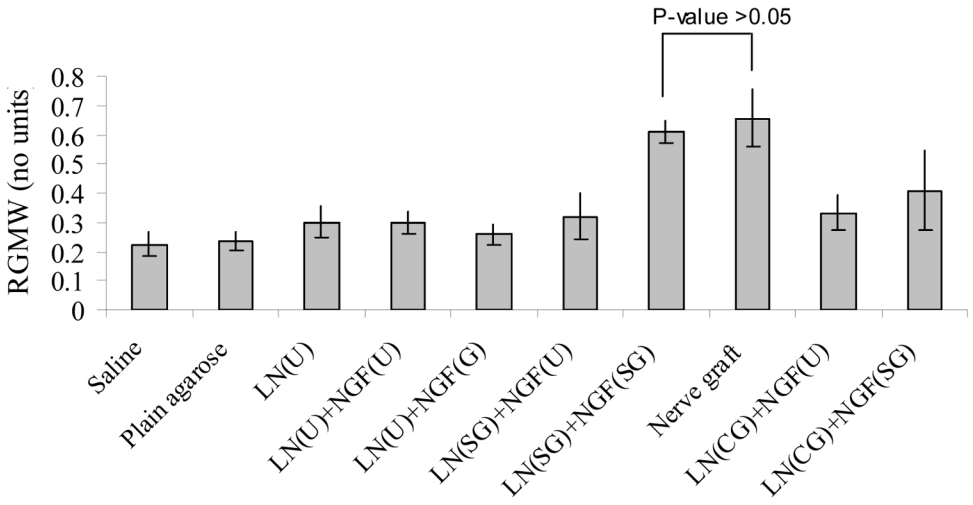

Figure 12.

Relative gastrocnemius muscle weight. Implants with step-gradients and nerve grafts had comparable RGMW (p-value > 0.05). The rest of the implant groups had significantly lower RGMW. All error bars indicate standard error of mean.

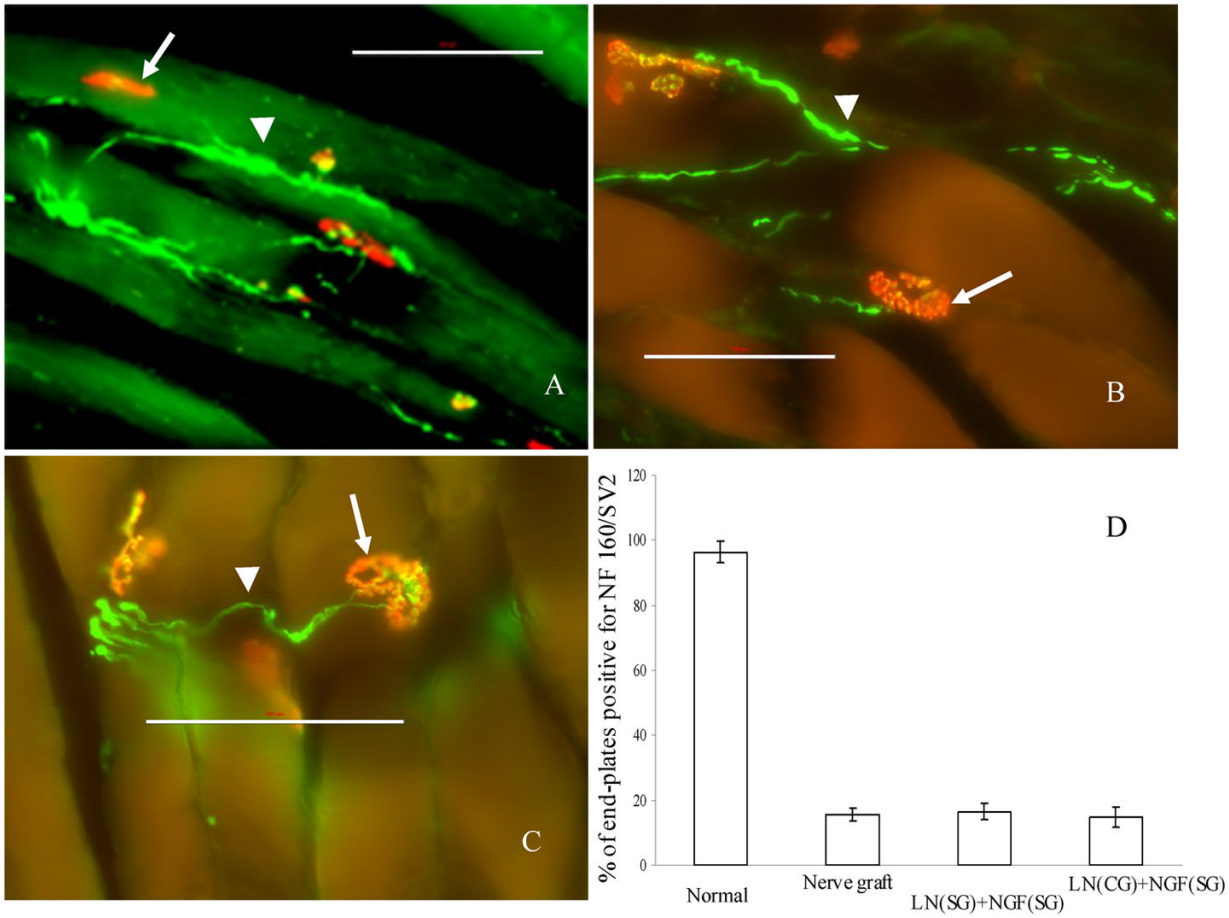

Figure 13.

Staining for acetylcholine receptors (AChR), synaptic vesicles (SV2) and neurofilaments (NF). All the three conditions: step-gradient scaffolds (A), continuous-gradient scaffolds (B) and nerve grafts (C); had neuro-muscular junctions positive for AChR (arrow), NF 160 (arrow-head) and SV2. All the NMJs in the figure panels are positive for SV2, to different degrees. The % of positive NMJs in the three conditions was similar, but much lower than that of a normal rat (D). Scale bar = 100 μm.

Table 1

Notation of experimental and control groups

Groups	Notation of groups	Components	# of rats
Control I (negative)	Saline	PBS solution	5
Control II (negative)	Plain agarose	0.5% agarose gels (no LN-1)	5
Control III (negative)	LN(U)[1]	*Isotropic* LN-1-agarose gels	5
Control IV (positive)	Nerve graft	Nerve grafts explanted from other Fischer inbred rats	8
Experimental I	LN(U)-NGF(U)	*Isotropic* LN-1-agarose gels embedded with *isotropic* NGF-loaded LMTs	10
Experimental II	LN(U)-NGF(SG)[2]	*Isotropic* LN-1-agarose gels embedded with *anisotropic* NGF-loaded LMTs	9
Experimental III	LN(SG)-NGF(U)	*Anisotropic* LN-1-agarose gels embedded with *isotropic* NGF-loaded LMTs	11
Experimental IV	LN(SG)-NGF(SG)	*Anisotropic* LN-1-agarose gels embedded with *anisotropic* NGF-loaded LMTs	
Experimental V	LN(CG)[3]-NGF(U)	*Anisotropic* LN-1-agarose gels embedded with *isotropic* NGF-loaded LMTs	7
Experimental VI	LN(CG)-NGF(SG)	*Anisotropic* LN-1-agarose gels embedded with *anisotropic* NGF-loaded LMTs	8

(U)[1] = uniform concentration,

(SG)[2] = step-gradient,

(CG)[3] = continuous-gradient

Table 2

Summary of nerve regeneration in control and experimental groups

Groups	Total # of rat	# of rats with regeneration	% regeneration
Saline	5	0	0
Plain agarose	5	0	0
LN(U)[1]	5	0	0
LN(U)+NGF(U)	10	0	0
LN(U)+NGF(SG)[2]	9	0	0
LN(SG)+NGF(U)	11	0	0
LN(SG)+NGF(SG)	**9**	**4**	**44.4**
LN(CG)[3]+NGF(U)	7	0	0
LN(CG)+NGF(SG)	**8**	**3**	**37.5**
Nerve graft	**6**	**5**	**83.3**

(U)[1] = uniform concentration,

(SG)[2] = step-gradient,

(CG)[3] = continuous-gradient